**"Supporting Information"**

# Altered phase behavior of the lauric acid-stearic acid binary mixtures in electrospun PVA-PDMS mats

*Shama Perween* [a], *Amit Ranjan* [a,]*

[a] Department of Chemical Engineering, Rajiv Gandhi Institute of Petroleum Technology, Jais, Uttar Pradesh, 229304, India.

**CORRESPONDING AUTHOR: Amit Ranjan* (*Email: aranjan@rgipt.ac.in)**

## S.1 CHARACTERIZATION METHOD & TECHNIQUE USED

### S.1.1. FE-SEM/ EDS/ AFM/ X-RAY DIFFRACTION/ FTIR/ RAMAN SPECTROSCOPY

The electrospun as-deposited nanofibrous composite mats were directly used to characterize the sample after drying at RT. The morphologies were imaged by using Field Emission Scanning Electron (FE-SEM) Microscopy (Zeiss Supra 40). The chemical composition was verified by elemental analysis on a Zeiss electron microscope (accelerating voltage ranged from 5 to 20 kV) equipped with an EDS analyzer. To prevent samples from charging, a thin gold coating was sputtered onto the samples prior to the analysis. Atomic Force Microscopy (AFM) imaging was carried out by Nanosurf AFM system in tapping mode using Dyn190Al cantilevers having a resonance frequency of around 190 kHz and a force constant of 48 N/m. The electrospun as-deposited samples were used for analysis done at RT. X-ray diffraction was carried out on a PANalytical X'pert Pro MPD diffractometer with monochromatic Cu Kα radiation (λ = 1.54056 Å) to investigate the phase changes and crystallinity. The Perkin Elmer Spectrum Two FT-IR spectrometer was used to record the FT-IR spectra of the

electrospun as-deposited nanofibrous composite mats. All the samples were recorded by using “attenuated total reflectance” (ATR) mode. The PIKE MIRacle single reflection horizontal ATR accessory equipped with a ZnSe ATR crystal was used for recording the FT-IR spectra. Raman images and spectra were recorded by a Confocal Raman Microscope, WITec using an alpha 300 RA equipped with a CCD camera, a UHTS spectrometer, Diode laser used for 532 nm excitation, Zeiss 50x air objective (Numerical aperture = 0.75) at -61°C.

### S.1.2. DIFFERENTIAL SCANNING CALORIMETRY

The differential scanning calorimetry (DSC) data of the samples were recorded on a DSC Q200 from TA Instruments under $N_2$ atmosphere (50 mL/min). Pre-weighed (~1.5 mg) as-deposited electrospun fibrous samples were taken in a $T_{zero}$ Aluminum pan for the measurement. The samples were heated from 25 to 85°C, cooled to 25°C, and again heated to 85°C at a rate of 2°C/min. The data obtained from the first and the second heating traces of the samples are reported in this article. The phase diagram has been drawn by using the DSC thermal transitions data. The largest variation in enthalpy measurements was found to be ±2% and the maximum deviation in temperature measurements was ± 0.10°C.

### S.1.3 ELECTROSPINNING (EMULSION ELECTROSPINNING TECHNIQUE)

Nanofibers mats were fabricated by using the mixture solution of a binary mixture of LA-SA, PVA, and PDMS in the electrospinning setup purchased from E-Spin Nanotech Pvt. Ltd, India. The final spinning solution was filled in a 10 mL plastic syringe having a stainless-steel needle at the tip. During the electrospinning, a positive high voltage of 15 kV was applied to the needle, and the fibers were collected on an aluminum foil wrapped around an electrically grounded rotating collector drum as a cathode. The needle-to-collector distance was kept in the range of 10-12 cm and the solution flow-rate was maintained by using a

syringe pump. The temperature and the relative humidity of the spinning chamber were respectively (26 ± 0.1)°C and (40 ± 1)%.

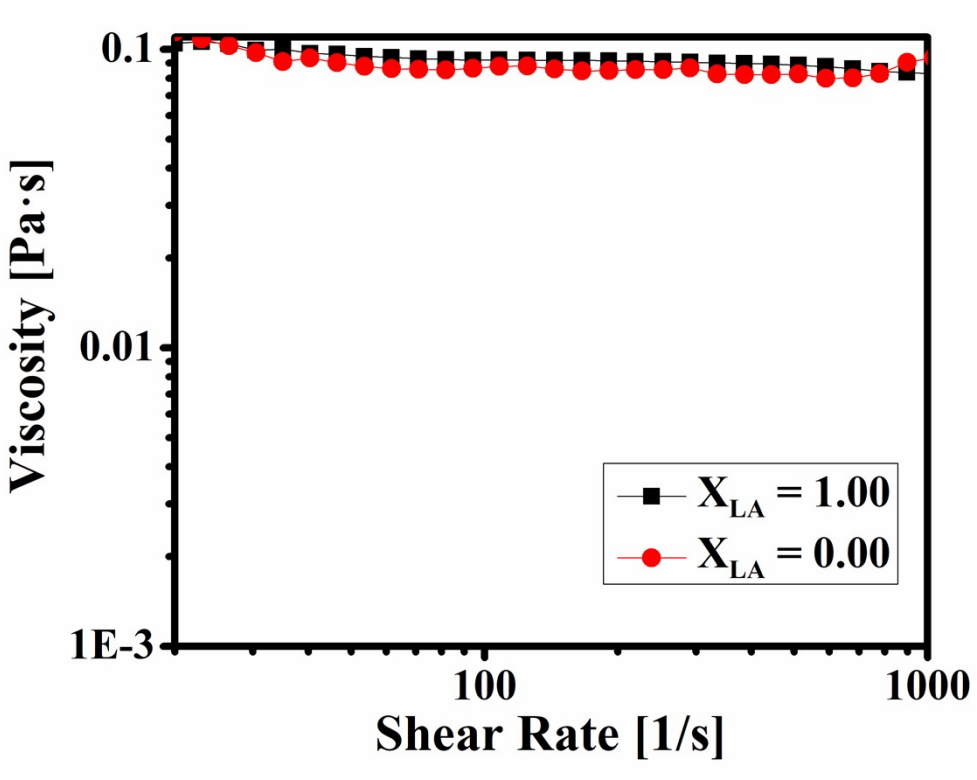


**Figure S1.** Rheology of LASA with PVA-PDMS spinning solution.

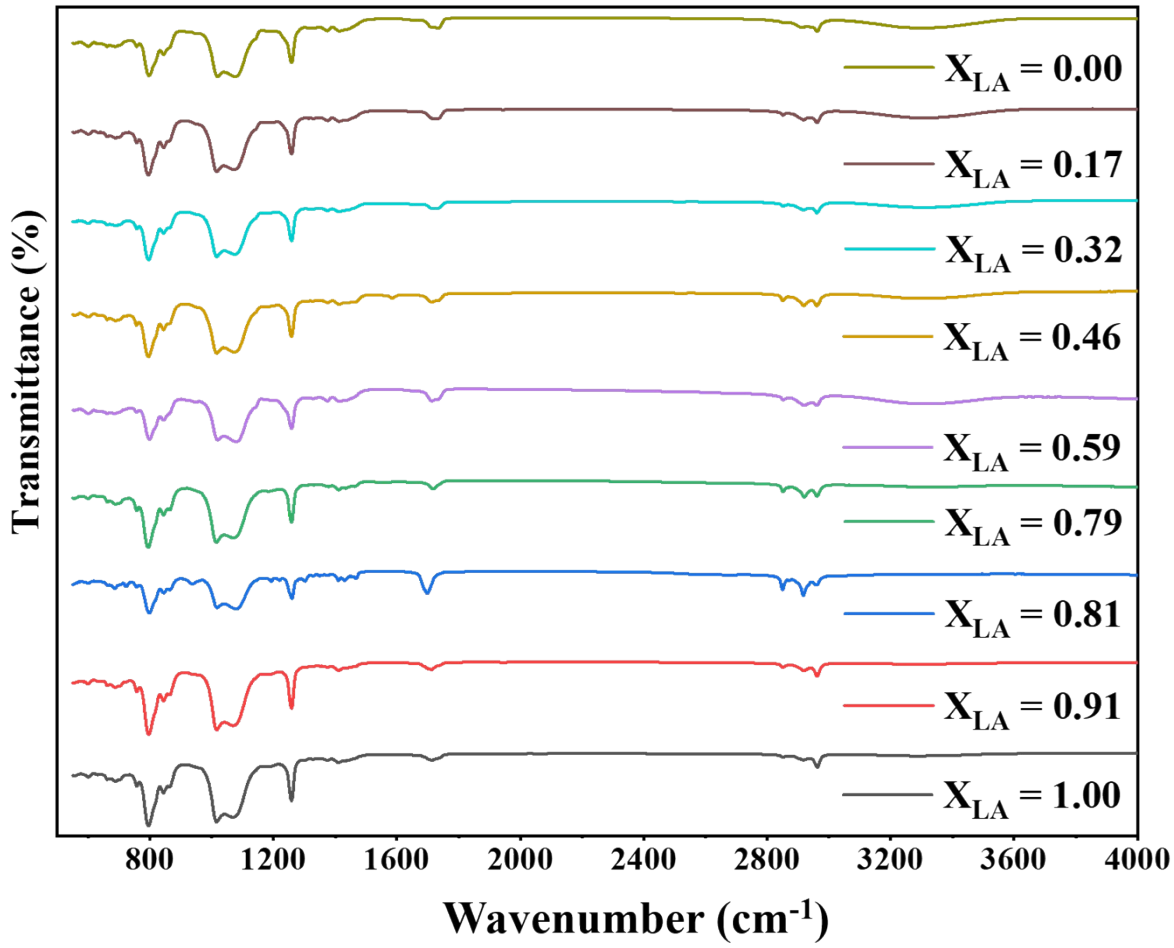


**Figure S2.** FT-IR spectra of as electrospun deposited mat with all composition of LASA mixtures in PVA-PDMS

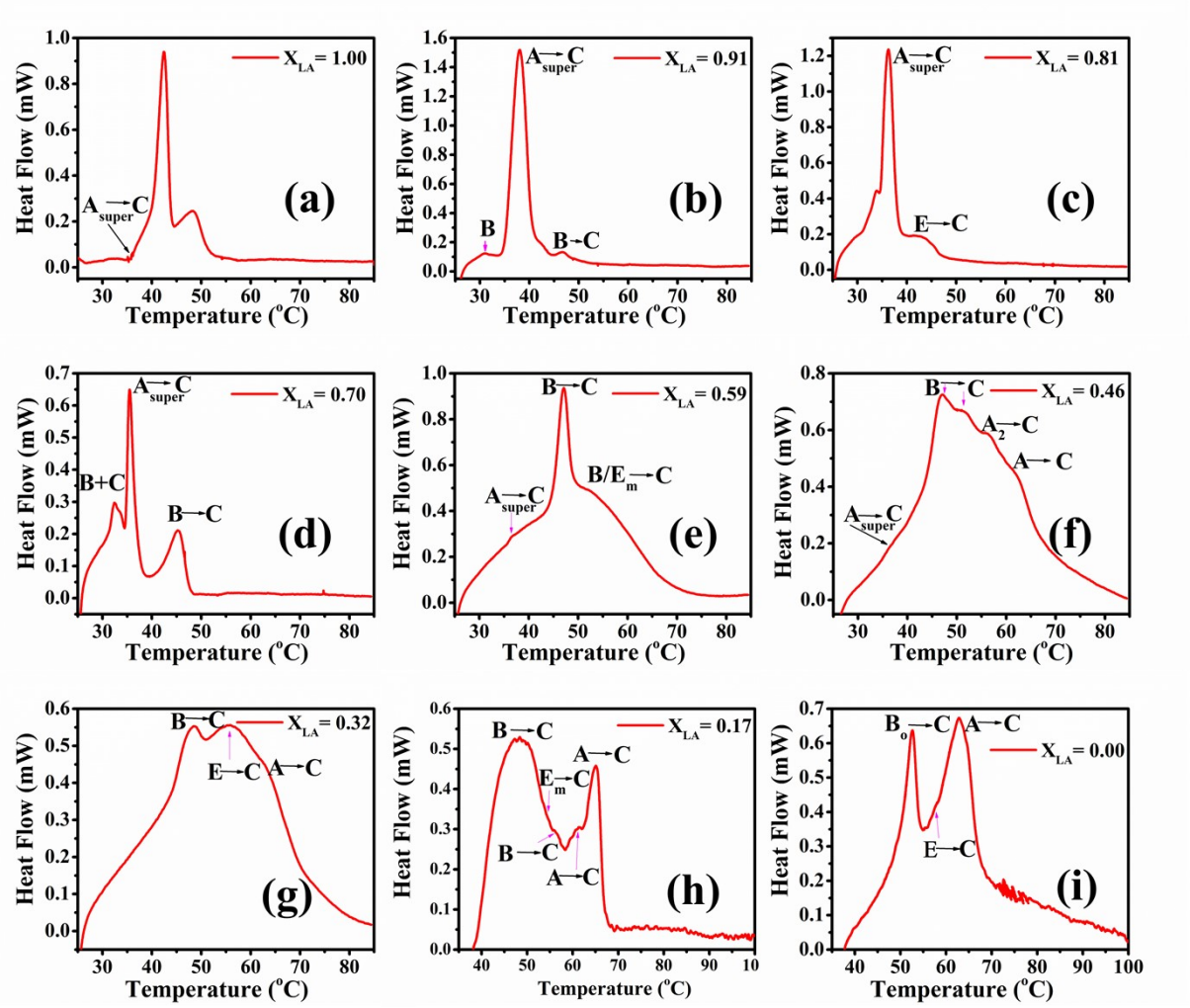


**Figure S3.** DSC heating scan with solid-solid transitions to the C-form of polymorphs of LASA of as electrospun deposited mat with all composition of LASA mixtures in PVA-PDMS.

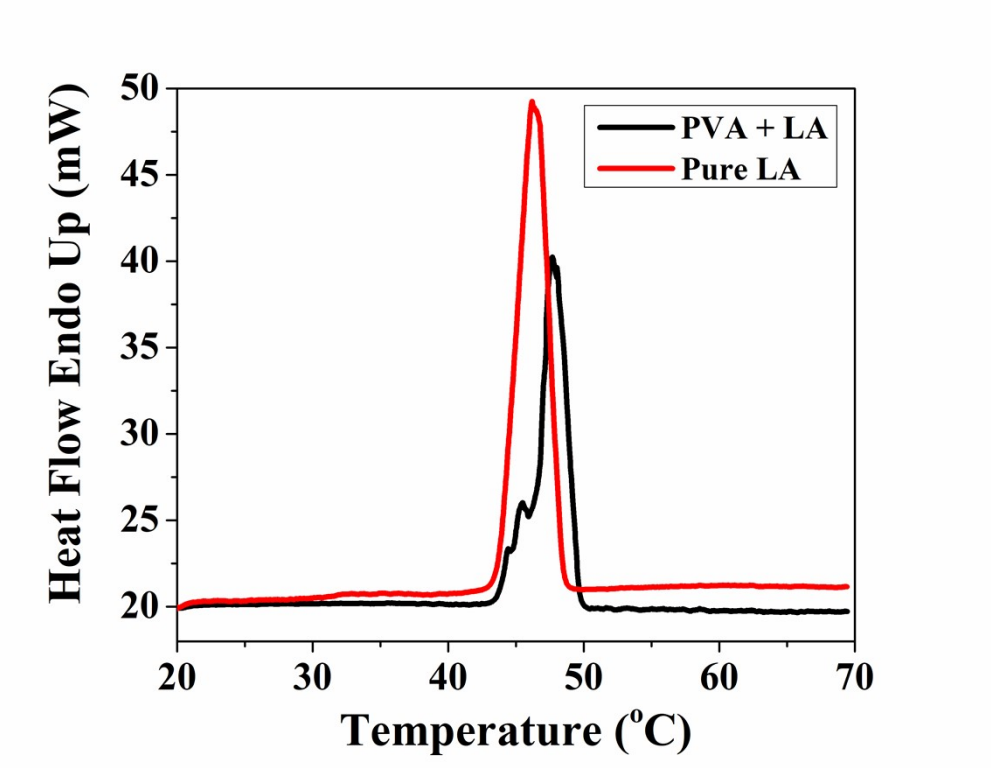


**Figure S4.** DSC heating scan of pure LA and mixture of PVA and LA.

**Table S1:** XRD diffractograms with corresponding planes of each molecule of PVA, LASA, and PDMS into the electrospun mat.

| Phases present in the spun mats | | Bragg's reflection angle (2θ) | Corresponding planes |
|---|---|---|---|
| Crystalline PVA | | 16° | (0 0 1) |
| | | 19.4° | (1 0 1) |
| | | 20° | (1 0 -1) |
| | | 22.7° | (2 0 0) |
| SA Polymorphs | E & $A_2$ | 6.6° | -- |
| | $A_{super}$ & B | 11.1° | (0 2 0) |
| | $E_m$ | 21.6° | (1 1 8) |
| | $E_o$ | 24.1° | (2 0 0) |
| LA Polymorphs | $A_{super}$ & C | 8.78° | (0 2 0) |
| | $A_{super}$ | 10.1° | (0 1 -3) |

| | | | |
|---|---|---|---|
| | $B_o/B_m$ | 19.6° | (1 1 5) |
| | $E_o$ & $B_o$ | 22.14° | (2 0 0) |
| | $E_m$ | 23.84° | (1 1 12) |
| | $E_o$ & $B_o$ | 24.8° | (2 0 0) |
| PDMS | | ~12º | -- |

**Table S2:** Solid-solid melting transitions and corresponding enthalpies.

| **Solid-solid transitions** | **Transition temperature (°C)** | **References** |
|---|---|---|
| LA (PVA/PDMS present) | 31.77 | This work. |
| LA (PVA/PDMS present) | 42.43 | This work. |
| LA (PVA/PDMS present) | 48.30 | This work. |
| $A_{super}$ (LA) to C form | 35.1 | E. von Sydow, *Ark. Kemi.*, 1956, 9, 231. |
| B (LA) ) to C form | 10.1 | G. L. Clark, Applied X-Ray, McGraw-Hill, New York, 1955. |
| B (LA) melting | 9.95 | |
| LA melting to C-form | 43.2 ± 0.4 | Moreno et al, *New J. Chem*., **2007**, *31*, 947–957. |
| LA melting to C-form | 45 | A. D. Bond, *New J. Chem*., **2004**, *28 (1)*, 104. |
| LA melting to C-form | 44.1 | Kobayashi et al, *Cryst. Liq. Cryst*., **1984**, 104, 193. |
| LA to C-form | 43.9 ± 0.1 | Vand *et al*, *Acta Crystallographica* , **1951**, *4 (4)*, 324-329; E. Stenhagen and E. von Sydow, *Ark. Kemi.*, **1952**, *6(29)*, 309; Moreno et al, *New J. Chem*., **2007**, *31*, 947–957. |
| LA to C-form | 44.2 ± 0.1 | Moreno et al, *New J. Chem*., **2007**, *31*, 947–957. |

| | | |
|---|---|---|
| B (SA) to C-form | 32 | Sato et al, *Journal of Crystal Growth* **1985**, *72*, 699-704; Sato, *Food Microstructure*, **1987**, *6*, 151-159. |
| | 46 | E. Stehagen and E. von Sydow, Arkiv Kemi **1953**, *6*, 309. |
| | 49 | Beckmann et al, *Journal of Crystal Growth*, **1986**, *74*, 326-330; Sato and Boistelle, *Journal of Crystal Growth* **1984**, *66*, 441—450 |
| | 54 | N. Garti. E. Wellner and S. Sang. Kristall Tech. **1980**, *15*, 1303; K.S. Kunihisa, *Thermochim. Acta* **1970**, *30*, 1. |
| A (SA)-form to C-form | 54 | E. Stehagen and E. von Sydow, Arkiv Kemi **1953**, *6*, 309. |
| | 64 | N. Garti. E. Wellner and S. Sang. Kristall Tech. **1980**, *15*, 1303. |
| SA | ~58.45 | This work. |
| $A_2$ (SA) to C-form | 58.6 | Moreno et al, *New J. Chem.*, **2007**, *31*, 947–957. |
| SA | 53.94, 63.85 | This work. |
| A (SA) to C-form | 54.1 | E. Stenhagen and E. von Sydow, *Ark. Kemi.*, **1952**, *6(29)*, 309. |
| $A_2$ (SA) to C-form | 58.6 ± 0.2 | Moreno et al, *New J. Chem.*, **2007**, *31*, 947–957. |
| A (SA) to C-form | 54.1 | E. Stenhagen and E. von Sydow, *Ark. Kemi.*, **1952**, *6(29)*, 309. |
| A (SA) to C-form | 64.1 | K. Sato and M. Kobayashi, *Crystals 13*, Springer-Verlag, Berlin, **1991**. |
| $E_m$ (SA) to C-form | 54.4 ± 0.6 | Moreno et al, *New J. Chem.*, **2007**, *31*, 947–957. |
| E (SA) to C-form | 43.6 | K. Sato and M. Kobayashi, *Crystals 13*, Springer-Verlag, Berlin, **1991**. |
| $B_m$ (SA) to C-form | 51.4 ± 0.7 | Moreno et al, *New J. Chem.*, **2007**, *31*, 947–957. |

| | | |
|---|---|---|
| $B_o$ (SA) to C-form | 52.9 ± 0.5 | |
| B (SA) to C-form | 51.1 | K. Sato and M. Kobayashi, *Crystals 13*, Springer-Verlag, Berlin, **1991**. |
| B (SA) to C-form | 55.1 | G. L. Clark, Applied X-Ray, McGraw-Hill, New York, 1955. |
| $E_m$ (SA) | ~54.25 | This work |
| E (SA) | 32.85 | |
| $B_m$ (SA) | ~51.25 | |
| $B_o$ (SA) | ~52.75 | |
| B (SA) | 50.95, 54.95, 45.95 | |

**Table S3:** Melting peaks of LA-SA in PVA-PDMS mats from 2nd DSC heating scans.

| **Mole fraction of LA ($X_{LA}$)** | **Mass fraction (LA)** | **Eutectic transitions (°C)** | **Solid-solid transitions-1 (°C)** | **Solid-solid transitions-2 (°C)** | **Solid-solid transition-3 (°C)** | **Solid-liquid transition-1 (°C)** |
|---|---|---|---|---|---|---|
| 1 | 1 | -- | -- | -- | 40.6432 | 46.48485 |
| 0.9082 | 0.875 | 33.23825 | -- | -- | 35.69391 | -- |
| 0.8098 | 0.75 | 32.67 | -- | -- | 37.98491 | -- |
| 0.7029 | 0.625 | 31.75 | -- | -- | 38.78309 | -- |
| 0.5867 | 0.5 | 31.95 | 39.68712 | 44.18329 | 49.38468 | -- |
| 0.46 | 0.375 | 32.22 | 44.45541 | 49.11414 | 54.88322 | 59.55281 |
| 0.3214 | 0.25 | 32.52 | 43.5572 | -- | 49.85541 | 59.62295 |

| | | | | | | |
|---|---|---|---|---|---|---|
| 0.16865 | 0.125 | 49.6889 | 60.26511 | -- | 64.82774 | 67.94 |
| 0 | 0 | 49.15667 | 50.17645 | 51.48513 | 61.22036 | 66.85 |